JACS
JOURNAL OF THE AMERICAN CHEMICAL SOCIETY
Article
pubs.acs.org/JACS

The Bacterial Ammonia Lyase EncP: A Tunable Biocatalyst for the Synthesis of Unnatural Amino Acids

Nicholas J. Weise, Fabio Parmeggiani, Syed T. Ahmed, and Nicholas J. Turner*

Manchester Institute of Biotechnology & School of Chemistry, University of Manchester, 131 Princess Street, M1 7DN Manchester, United Kingdom

Supporting Information

ABSTRACT: Enzymes of the class I lyase-like family catalyze the asymmetric addition of ammonia to arylacrylates, yielding high value amino acids as products. Recent examples include the use of phenylalanine ammonia lyases (PALs), either alone or as a gateway to deracemization cascades (giving (*S*)- or (*R*)-*α*-phenylalanine derivatives, respectively), and also eukaryotic phenylalanine aminomutases (PAMs) for the synthesis of the (*R*)-*β*-products. Herein, we present the investigation of another family member, EncP from *Streptomyces maritimus*, thereby expanding the biocatalytic toolbox and enabling the production of the missing (*S*)-*β*-isomer. EncP was found to convert a range of arylacrylates to a mixture of (*S*)-*α*- and (*S*)-*β*-arylalanines, with regioselectivity correlating to the strength of electron-withdrawing/-donating groups on the ring of each substrate. The low regioselectivity of the wild-type enzyme was addressed via structure-based rational design to generate three variants with altered preference for either *α*- or *β*-products. By examining various biocatalyst/substrate combinations, it was demonstrated that the amination pattern of the reaction could be tuned to achieve selectivities between 99:1 and 1:99 for *β*:*α*-product ratios as desired.

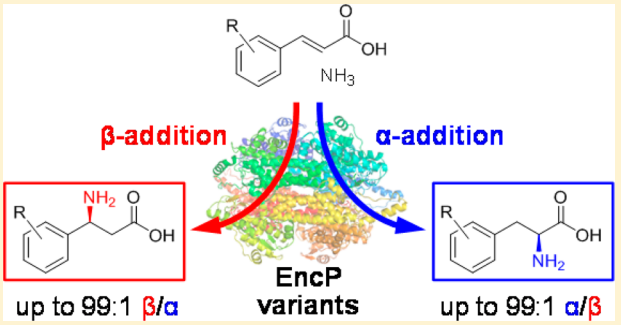

INTRODUCTION

Unnatural or nonproteinogenic amino acids are an important class of compound in medicinal chemistry as evidenced by their presence in numerous natural products with potent bioactivities.[1,2] As such, amino acids are used as chiral building blocks for the synthesis of both pharmaceuticals and lead compounds in drug discovery.[3−5] There are also promising efforts to incorporate unnatural amino acids into proteins and peptide mimics as tools in chemical biology[6,7] or to improve their therapeutic properties.[8,9] Because of the prevalence of amino acid metabolizing enzymes in nature, biocatalysis represents an attractive strategy to develop greener and more generally applicable routes to these compounds.

The class I lyase-like family is a group of structurally and mechanistically related enzymes, which, in nature, catalyze the deamination of aromatic amino acids to yield the corresponding arylacrylic acids. Enzymes that proceed no further than this are known as ammonia lyases (ALs) and can be histidine (HAL - EC 4.3.1.3), phenylalanine (PAL - EC 4.3.1.24/25), or tyrosine (TAL - EC 4.3.1.23/25) specific. Other family members also allow subsequent reamination at the *β*-position (aminomutases or AMs), thus catalyzing overall *α*- to *β*-isomerization of phenylalanine (PAM - EC 5.4.3.10/11) or tyrosine (TAM - EC 5.4.3.6).[10,11]

PALs and PAMs have been shown to accept many ring-substituted cinnamate derivatives as substrates for amination reactions, making them the most broadly applicable family members for development as biocatalysts. Use of PALs includes

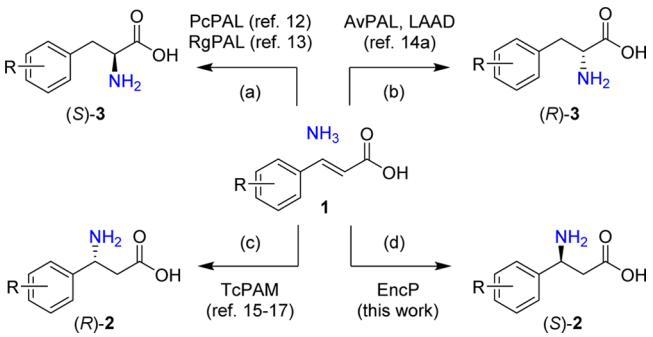

Figure 1. Complete PAL/PAM toolbox for production of either enantiomer of *α*-phenylalanine derivatives (a,b) and *β*-phenylalanine derivatives (c,d) from the corresponding acrylic acids.

both small- and industrial-scale (*S*)-selective *α*-amination of halocinnamates using enzymes from *Petroselinum crispum*[12] and *Rhodotorula glutinis*,[13] respectively (Figure 1a). Recently, we reported an enantiocomplementary route to the (*R*)-*α*-arylalanines, which exploits the imperfect enantiopreference of AvPAL (from *Anabaena variabilis*) in combination with an L-amino acid deaminase and chemical reduction as a deracemization step (Figure 1b).[14] Work by Janssen et al. has focused on the characterization and engineering of an (*R*)-selective aminomutase from *Taxus wallichiana* var. *chinensis* to access

Received: July 14, 2015
Published: September 21, 2015

DOI: 10.1021/jacs.5b07326
J. Am. Chem. Soc. 2015, 137, 12977−12983

enantiopure (*R*)-*β*-phenylalanine derivatives (Figure 1c).[15−17] This leaves only the (*S*)-*β*-aromatic amino acids, which cannot be produced via direct amination with current methods (Figure 1d).

The enzyme EncP has been demonstrated to be a PAL in the thermotolerant bacterium *Streptomyces maritimus*, siphoning the primary metabolite phenylalanine into natural product biosynthetic pathways for enterocin and wailupemycin antibiotics.[18,19] More recent studies of this enzyme, along with the closely related AdmH from *Pantoea agglomerans* (63% sequence identity), revealed both enzymes to be thermobifunctional (displaying a decreased lyase:mutase ratio with increasing temperature).[20] Despite high sequence similarity, AdmH has been revealed to be an aminomutase physiologically, catalyzing the interconversion of (*S*)-*α*- to (*S*)-*β*-phenylalanine as a precursor for the peptide antibiotic andrimid.[21] As with all class I lyase-like enzymes, this unique amine chemistry is mediated by the family-specific 4-methylideneimidazole-5-one (MIO) prosthesis. The electrophilic MIO moiety is formed post-translationally in the active site by cyclization and dehydration of the tripeptide [AT]SG, and is suggested to bind and release the primary amine/ammonia covalently, as required for (re)amination or deamination (Figure 2).[10,11] The active site

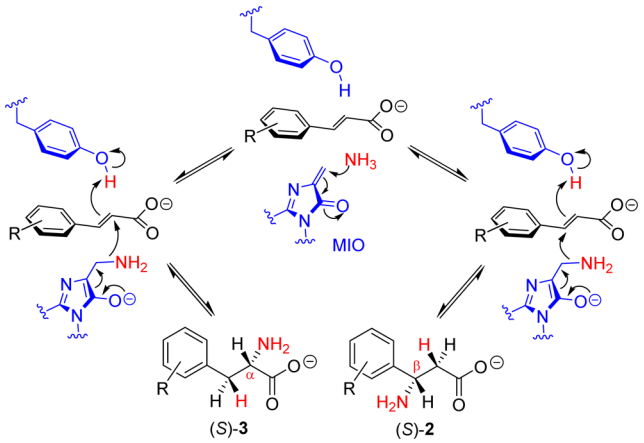

Figure 2. Catalytic mechanism of the proposed (*S*)-selective MIO-dependent amination of cinnamate derivatives.

geometry of AdmH has been demonstrated to limit the phenylalanine isomerization reaction to a single rotamer of the cinnamate intermediate, with the MIO catalyzing amination/deamination on the same face, thus giving the particular stereochemistry of *β*-amination.[22] As neither of these enzymes (with proven or predicted (*S*)-selective aminomutase activity) has been investigated in the amination direction, EncP was selected as a template for the development of the missing biocatalyst in the PAL/PAM toolbox (Figure 1).

A pET expression vector containing the codon-optimized gene encoding the EncP protein[20] was used to transform *E. coli* BL21(DE3) cells according to standard procedures. The biocatalyst was then prepared via autoinduction on an 800 mL scale,[14] yielding wet whole cells. Protein overproduction was confirmed via polyacrylamide gel electrophoresis of denatured protein fractions following nickel affinity chromatography. Initial testing of the whole cell catalyst under previously reported conditions for AvPAL[14] and *Taxus* PAM[15] gave no detectable activity with cinnamate **1a** as a substrate, ascertained via HPLC on a nonchiral phase in comparison with authentic standards. After different ammonium salts were sampled and buffer pH and incubation temperature were changed (Tables S1−S4), a method was developed by which ∼80% conversion of 1 mM cinnamate could be observed after a 22 h reaction period. As such, the following method was applied to all subsequent analyses: 40 mg mL^{-1} whole cells in 4 M $(NH_4)_2SO_4$ (pH 8.3), 55 °C, 550 rpm, 22 h.

Initially a panel of cinnamate derivatives **1a−v** was subjected to biotransformations with EncP-overproducing *E. coli* BL21(DE3) cells. Formation of the corresponding amino acids **2−3a−v** was monitored by HPLC (Figure 3) revealing that the enzyme was able to convert all 22 substrates tested. Interestingly, conversions tended to follow the pattern *ortho-* > *meta-* > *para-*, with most *ortho*-substituted cinnamates showing conversion greater than or equal to that of the unsubstituted "natural" substrate **1a**. There was also little disparity between the conversions achieved with all of the *ortho*-substituents regardless of size, with *para-* and to a lesser extent *meta*-substituted substrates displaying decreased conversions with increasing substituent bulkiness. This substrate profile is in contrast to that reported for the *Taxus* PAM reaction, where *para*-substituents are converted with higher efficiency and larger *ortho-* and *meta*-products do not appear to be tolerated.[15] This difference is likely due to the cinnamate being bound in alternate orientations within the active sites of (*S*)- and (*R*)-selective PAMs, as is evident from their overlaid crystal structures.[23] The methoxycinnamates **1p−r** do not seem to follow this pattern with the lower than expected conversion of the *ortho*-isomer, possibly due to steric clash of this bulky group with the activated *β*-carbon.

The regioselectivity was also found to be affected by the ring substituents with respect to their electron-withdrawing/donating nature, position, and number. As compared to cinnamate **1a**, which gave only a slight excess of *β*-product, it was found that nitro groups anywhere on the aromatic ring gave predominantly *α*-amino acids. Of these, 2- and 4-nitro- **1m** and **1o** gave much less of the *β*-isomer than 3-nitro- **1n**, which clearly suggests resonance effects. The halogenated compounds **1b−l** also exhibited increased *α*-selectivity with *ortho-* (and to a lesser extent *meta-*) substituents. The number of electron-withdrawing groups was found to have an effect, as seen with the increase in *α*-product between 3-fluoro-, 3,5-difluoro-, and 2,3,4,5,6-pentafluorocinnamate (**1c,e,f**). An increased excess of *β*-amino acid was displayed with all electron-donating substituents, with the exception of 2-methylcinnamate **1s**. The methoxycinnamates **1p−r** showed mirrored regioselectivity to the nitrocinnamates **1m−o**, also implying resonance effects. Oddly, the 4-halocinnamates (**1d,i,l**) also showed an increase in *β*-production relative to *α*-production.

To probe the contribution of electronic effects to the regioselectivity of the amination reaction, substituent- and position-specific core electron binding energy shift (ΔCEBE) values[24] were plotted against the percentage *β*-product of each reaction (Figure 4). These calculated values are described to be a measure of the difference in energy required to remove an electron from the *ipso*-carbon of a substituted aryl ring as compared to the unsubstituted *π*-system. As such, ΔCEBE was used as a quantitative measure of the electron richness/deficiency of the aromatic ring of each substrate, and therefore its relative ability to activate the molecule for ammonia addition as compared to the carboxyl moiety. There was a strong negative correlation, consistent with either the conjugate

DOI: 10.1021/jacs.5b07326
J. Am. Chem. Soc. 2015, 137, 12977−12983

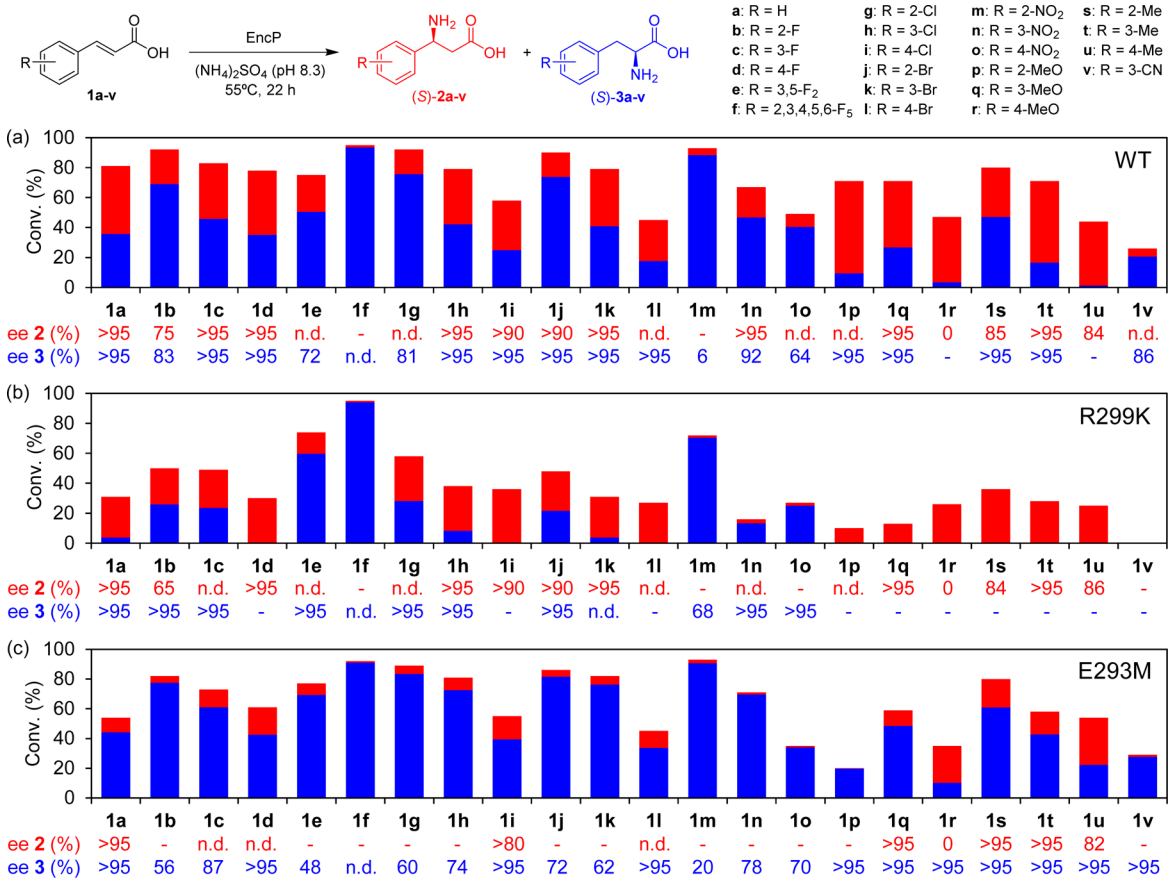

Figure 3. Amination of arylacrylic acids **1a–v** to the corresponding amino acids by EncP and two rationally designed, regioselective variants (n.d. = not determined, – = not required).

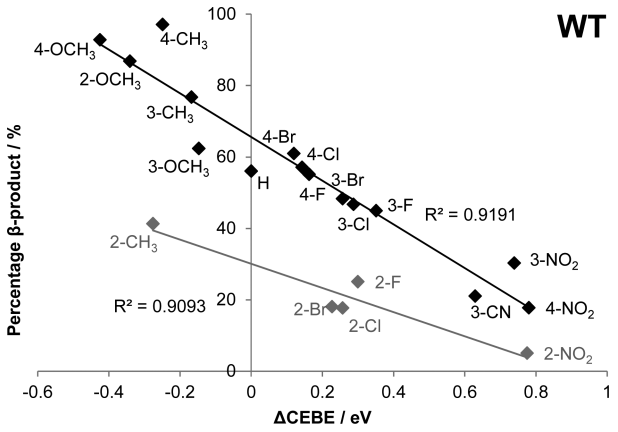

Figure 4. Dependence of β- versus α-amination by EncP on the core electron binding energy shift (ΔCEBE) due to substrate ring substituents.

addition[17] or the concerted hydroamination mechanism,[25] previously proposed for related aminomutases.

The data points were best fitted by two trend lines: one shallower in gradient through the majority of the *ortho*-substituents and the other through the remaining substrates, possibly indicating different binding modes in the active site. It is noteworthy that 2-methoxycinnamate **1p** is the only *ortho*-substituted compound to give an amination pattern that fits with the steeper trend line. These observations (along with additional deviations, such as increased β-selectivity for the electron-deficient 4-halocinnamate rings) imply that the specific interactions of each substrate with the active site contribute to reaction parameters, as was recently proposed for amino acid isomerization reactions with AdmH.[25] In fact, it could be reasoned that interactions of ring substituents with the active site may affect the positioning of each substrate. For example, the orientation of *ortho*-groups relative to the rest of the substrate might enable different accommodation of these by the aryl binding pocket of the enzyme, as compared to the elongated *meta*- and *para*-analogues. This may impact upon positioning of the β- and α-carbons relative to the catalytic residues and contribute to the differing trends in amination preference observed with these subsets of compounds.

As expected, the amination reaction was found to yield predominantly the (*S*)-amino acids ((*S*)-**2** and (*S*)-**3**) for the majority of substrates (Figure 3). In many cases, good to excellent ee values were obtained, with nine examples of completely stereoselective addition at both β- and α-positions. The ee of the α-products **3m–o** for the nitrocompounds was imperfect, with 2-nitrocinnamate **1m** (the highest converted of the three) giving a particularly low value of just 6% ee for **3m**. This low ee may be due to a competing MIO independent amination process previously observed with AvPAL,[14] allowing amination from either face of the substrate. Interestingly, the 4-methoxycinnamate **1r** was found to produce racemic **2r** under the reaction conditions. This outcome may be linked to the steric and electronic similarities between the 4-methoxyphenylalanines **2–3r** and tyrosine β- and α-regioisomers (4-OCH_3 vs 4-OH substituent). Tyrosine is disfavored by PAL and PAM

DOI: 10.1021/jacs.5b07326
J. Am. Chem. Soc. 2015, 137, 12977–12983

enzymes and may therefore not be correctly bound in the active site for stereoselective amination/deamination reactions.

The probable interplay of substrate binding versus electronic effects in EncP prompted rational design efforts to tailor regioselectivity for compounds with undesirable β:α ratios. A homology model of EncP was constructed using the structure of AdmH (PDB ID: 3UNV)[23] as a guide (Figure 5 and Figures

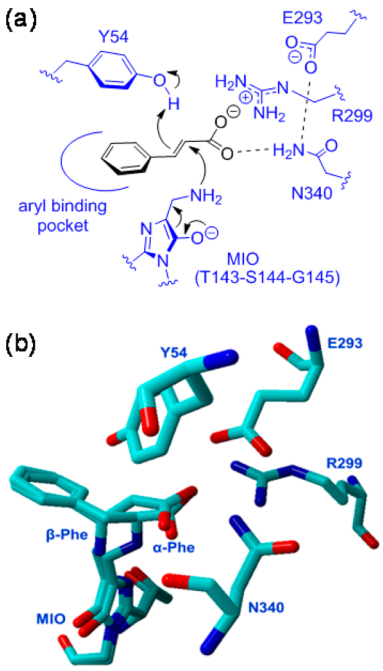

Figure 5. EncP active site catalytic and substrate positioning residues as inferred by homology modeling based on AdmH.

S1,S2). Residues considered to be important for substrate positioning were selected and point mutations designed. The most striking enzyme–substrate interactions in this model seemed to be a hydrogen bond (from N340) and a salt bridge (from R299) to the carboxyl group of the substrate (Figure 5a). Residues N340 and R299 seemed, in turn, to be coordinated by ionic and hydrogen-bonding interactions, courtesy of the neighboring E293. It was postulated that by substituting R299 and E293 in EncP the nature of these interactions could be altered, shifting the positioning of the substrate in the active site and thus affecting the β- and/or α-addition preference.

Previous efforts aimed at engineering the carboxyl-binding pocket in a plant PAL have revealed a delicate hydrogen-bonding network, which is easily disturbed by mutagenesis.[26] For this reason, the original residues in EncP were substituted for amino acids with the highest similarity. Residue R299 was mutated to a K to maintain the charge interaction with the substrate, and this variant showed increased β-selectivity (from 56:44 to 88:12) with cinnamate **1a** (Figure 3). This change in selectivity could possibly be rationalized by the different shape and higher charge density of the lysine terminal amine (versus the arginine guanidinyl moiety) sliding the β-carbon of the substrate in a more central position for amination by the catalytic MIO and tyrosine residues (Figure 6b). Next the neighboring E293 was substituted for Q to generate a variant that displayed opposite regioselectivity, producing an excess of α-phenylalanine from **1a** (43:57). With little shape difference between glutamate and glutamine, the change in selectivity may be due to reduced interaction strength between positions 293

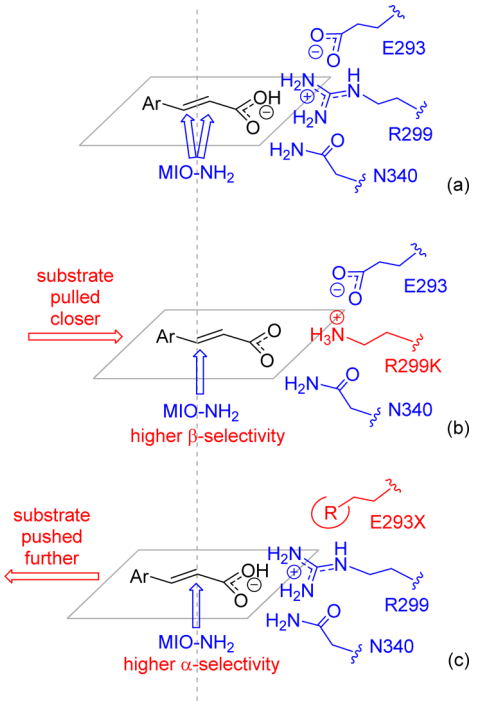

Figure 6. Hypothesized effect of varying active site residues on substrate positioning and ammonia addition preference.

and 299. By removing the salt bridge, here it is likely that R299 is repositioned, shuttling the substrate in the active site so as to allow easier α-amination versus β- (Figure 6c). This hypothesis was tested further with an E293M substitution, to remove any residual polar interactions between the two amino acid side chains. This variant displayed further improved α-selectivity (18:82) as compared to EncP-E293Q. To our knowledge, the E293 variants are the first examples of PAM enzymes with significantly increased α-selectivity achieved through enzyme engineering. Further details on the rational design are provided in the Supporting Information.

The regio- and stereoselectivity of each of the three variants was then tested with the entire panel of compounds **1a–v** under the same conditions as for the wild-type enzyme (Figures 3 and 7). EncP-R299K was found to convert all substrates with the exception of 3-cyanocinnamate **1v**, where no product was detected. For the majority of substrates a large increase in β-selectivity was observed, with nine substrates producing exclusively the β-amino acid (all three *para*-halocinnamates **1d**, **i**, and **l**, and all six methyl- and methoxy-compounds **1p–u**). Interestingly, the 3-fluoro- compound **1c** showed only a minor β-:α-product shift as compared to the other *meta*-halogenated substrates (45:55 to 52:48), causing it to remain on the upper wild-type trend line in the same region as the *ortho*-halocompounds (Figure 7). Apart from this cluster and the largely unaltered pattern for the nitro-products (**m–o**), the previously influential effect of substrate electronic effects seemed to have been greatly disrupted by the R299K amino acid substitution. Both EncP-E293Q and EncP-E293M showed conversion with the entire substrate panel, with increased α-selectivity in most cases. EncP-E293M in fact gave a β:α-product ratio of <30:70 with 20 of the 22 substrates (all except **1r** and **1u**). These 20 points were found to lie around or below the lower trend line for the wild-type reactions (Figure 7), indicating a similar but opposite disruption of the regioselecti-

DOI: 10.1021/jacs.5b07326
J. Am. Chem. Soc. 2015, 137, 12977–12983

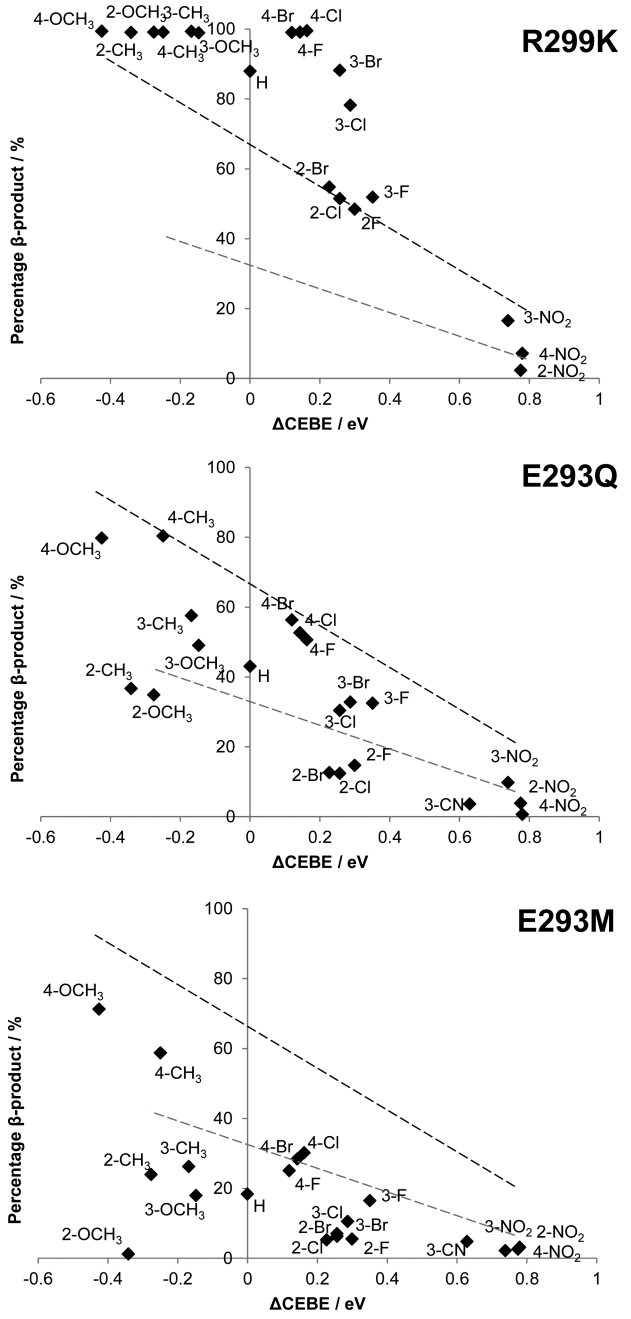

Figure 7. Dependence of β- versus α-amination by EncP rationally designed variants on the core electron binding energy shift (ΔCEBE) due to substrate ring substituents. Trends for the wild-type enzyme are shown as dashed lines for comparison.

vity−ΔCEBE correlation, as seen with the first variant. The changes observed for E293Q were more subtle (the results for conversions and enantioselectivity are given in Figure S7), with almost all *para*-substitutions remaining on or around the wild-type upper trend line (Figure 7). The majority of *meta*- and the unsubstituted compounds, however, had moved to an intermediary position on the graph, between the two original trend lines, with the remaining *ortho*- and 3-cyano- substrates lying close to the lower trend line. The previously "outlying" **1p** displayed a marked jump from β- to α-selectivity (β:α ratio from 87:13 to 37:63), having fully migrated between the two trend lines. Again, compounds with strongly electron-withdrawing groups (ΔCEBE > 0.6 eV) showed little change in regioselectivity with either E293 variant, as with the β-selective enzyme. This implies that a highly electron-deficient ring activates the α-carbon strongly enough to counteract any changes in substrate positioning we had hypothesized. By contrast, the greatest shift in regioselectivity was seen with 2-methoxycinnamate **1p**, which, despite lowered conversion, could be produced as either the β- or the α-amino acid with no detectable trace of the other regioisomer with EncP-R299K or EncP-E293M, respectively.

The enantioselectivity of the β-amination reactions across all variants was found to be similar for each substrate regardless of the differences in conversion and regioselectivities observed. By contrast, the ee values for α-amination were found to decrease for many of the substrates with increasing α-regioselectivity (R299K > WT > E293Q/M). With the β-selective EncP-R299K only one substrate (2-nitrocinnamate **1m**) gave the α-product (*S*)-**3m** with <95% ee, with all others showing no detectable trace of the opposite enantiomer. The more α-selective variants gave moderate to poor ee values with 10 of the 22 converted substrates, of which five were <60% (*S*) for E293Q and four for E293M.

As a further test of the enantioselectivity, a time course experiment was set up to follow the enantiomeric excess for conversion of **1s** to **2s** using the EncP-R299K variant (Figure 3) to see if an erosion of ee was observed for β-amination by EncP that was similar to that reported for α-amination in AvPAL.[14] After 48 h, it was found that, although conversion tailed off after the first 8 h, the enantiomeric excess of **2s** continued to fall (Table 1). Interestingly, this was found not to

Table 1. Time Course of the Amination of Methylcinnamate 1s to Methyl-β-phenylalanine 2s by the EncP-R299K Variant

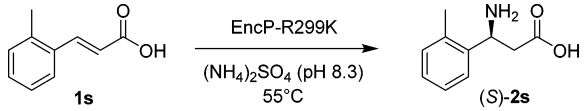

time (h)	conv. (%)[a]	β:α ratio[a]	ee of **2s** (%)[b]
1	10	99:1	>96
2	19	99:1	95
4	22	99:1	92
8	24	99:1	90
22	26	99:1	84
48	28	99:1	76

[a]Conversion and product ratios determined by nonchiral HPLC. [b]Enantiomeric excesses determined by chiral HPLC.

be the case with the *meta*- and *para*-isomers **2t−u** (Table S11). This may demonstrate a difference in the preference of the enzyme for the two possible binding modes of *ortho*-substituted arylacrylates, as previously alluded to by Walker et al.[25,27]

In summary, we have demonstrated that EncP can be engineered to enhance the regioselectivity of the addition of ammonia to cinnamic acid derivatives. The varying and often undesirable regioselectivity of the enzyme was found to be heavily influenced by the electronic properties of the substrates. Rational design of three EncP variants revealed that both the β- and the α-selectivity of the enzyme could be enhanced, allowing conversion to either (*S*)-β or (*S*)-α-arylalanines with 99:1 selectivity and high ee. Further engineering is currently underway to improve conversions for the β-products to fully develop a biocatalyst for the preparative synthesis of (*S*)-β-amino acids.

DOI: 10.1021/jacs.5b07326
J. Am. Chem. Soc. 2015, 137, 12977−12983

EXPERIMENTAL SECTION

General Methods and Materials. Analytical grade reagents and solvents were obtained from Sigma-Aldrich, AlfaAesar, or Fisher Scientific and used without further purification, unless stated otherwise. Reference standards of optically pure amino acids were purchased from Sigma-Aldrich, AlfaAesar, or PepTech Corp. Plasmid DNA purification was performed with the QIAprep Spin miniprep kit (Qiagen), according to the manufacturer's instructions. Automated DNA sequencing was performed by MWG Eurofins. *E. coli* DH5α was used as a cloning host for plasmid propagation, *E. coli* BL21(DE3) as an expression host for protein production. Chemically competent cells of both strains were purchased from New England Biolabs. Solid and liquid media were supplemented with kanamycin (50 μg mL^{-1} final concentration). Solid media were prepared by addition of agar (1.5% w/v) to liquid media. The pET-28a-EncP plasmid (pET-28a vector containing the codon-optimized gene encoding the EncP protein) was obtained from Prof. Jason Micklefield and used as previously reported.[20]

Molecular Visualizations and Modeling. The protein structure for the aminomutase AdmH[23] was downloaded from the Research Collaboratory for Structural Bioinformatics' Protein Data Bank – RCSB PDB (PDB ID: 3UNV). Homology models were created using the experiment option in the YASARA Structure version 14.7.17, with the "slow" modeling method. For this, the amino acid sequence of the query enzyme was input in FASTA format along with the unmodified PDB file for the appropriate structure. The number of PSI-BLAST iterations to build a position-specific scoring matrix from related sequences was set to 3 with an *E*-value cutoff of 0.5. Sequences profiles were obtained from YASARA's position specific scoring matrix (PSSM). The maximum number of top scoring templates was set to 5, with a maximum of 5 alignments per template and a maximum oligomerization state for templates of 4. The number of sampling experiments to optimize loop structures was set to 50 with a terminal extension value of 10. Side-chain rotamers were selected using electrostatic and knowledge-based packing interactions as well as solvation effects with implicit solvent. Hydrogen-bonding network was optimized to including pH-dependence and ligands bound via hydrogen prediction and visualization. A high-resolution energy minimization with a shell of explicit solvent molecules was run using YASARA version-specific knowledge-based force field parameters.

Site-Directed Mutagenesis of EncP. Specific mutations were introduced in the pET-28a-EncP template using the Phusion site-directed mutagenesis kit (Thermo Scientific) according to the protocol provided. The PCR reactions were performed on an Eppendorf Mastercycler Gradient using the following primers (mutated codon underlined): R299K_Fw = 5′-AGCATT<u>AAG</u>TGTACACCG-3′, R299K_Fw = 3′-CCGTTAACTTCTACGTATA-5′, E293Q_Fw = 5′-GGCAATT<u>CAG</u>GATGCATATAGC-3′, E293M_Fw = 5′-GGCAATT<u>ATG</u>GATGCATATAGC-3′, E293Q_Rv (=E293M_Rv) = 3′-CAACGTTTTCGTCCATCGGA-5′. PCR conditions: 98 °C (30 s), [98 °C (15 s), 58 °C (30 s), 98 °C (150 s)] × 30, 72 °C (300 s). Ligated PCR product or template plasmid was transformed into *E. coli* DH5α as per the manufacturer's protocol and grown on LB-agar plates for 16 h at 37 °C. Single colonies from these were used to inoculate LB cultures (5 mL) grown for 16 h at 37 °C (250 rpm shaking). Plasmid DNA was isolated and the presence of the mutation verified by automated DNA sequencing. The sample was then transformed into *E. coli* BL21(DE3) for protein production.

Whole Cell Biocatalyst Production. LB medium (8 mL, supplemented with kanamycin) was inoculated with a single colony of *E. coli* BL21(DE3) containing the suitable plasmid and grown for 16 h at 37 °C and 250 rpm. The starter culture was used to inoculate LB-based autoinduction medium[28] (800 mL, supplemented with kanamycin), which was incubated at 18 °C and 250 rpm for 4 days. The cells were harvested by centrifugation (4000 rpm, 12 min) and stored at −20 °C until further use. Protein overproduction was confirmed via SDS-PAGE analysis and by purification by immobilized metal affinity chromatography (Figure S3).

Optimized Biotransformation Procedure for the Amination of Substrates 1a–v. *E. coli* BL21(DE3) whole cells containing the PAL variant (40 mg wet weight) were resuspended in a solution of substrate **1a–v** (1 mM) and $(NH_4)_2SO_4$ (4 M, pH 8.3, 1.0 mL total volume). The mixture was incubated at 55 °C and 400 rpm for 22 h unless otherwise stated. Biotransformation samples were mixed with an equal volume of MeOH, vortexed, and centrifuged (13000 rpm, 3 min). The supernatant was transferred to a 0.45 μm filter vial and used directly for HPLC analysis. Methods and conditions are reported in the Supporting Information.

ASSOCIATED CONTENT

Supporting Information

The Supporting Information is available free of charge on the ACS Publications website at DOI: 10.1021/jacs.5b07326.

Figures S1–S7, Tables S1–S11, further experimental details, analytical methods, and additional data (PDF)

AUTHOR INFORMATION

Corresponding Author

*nicholas.turner@manchester.ac.uk

Notes

The authors declare no competing financial interest.

ACKNOWLEDGMENTS

This work was funded by the European Union's 7th Framework program FP7/2007–2013 under grant agreement no. 289646 (KYROBIO). F.P. and S.T.A. were supported by the Biotechnology and Biological Sciences Research Council (BBSRC) and Glaxo-SmithKline (GSK) under the Strategic Longer and Larger (sLoLa) grant initiative ref BB/K00199X/1. We thank the Royal Society for a Wolfson Research Merit Award (N.J.T.). We thank Professor Jason Micklefield and collaborators for providing the construct for production of EncP. Thanks also go to Scott P. France and Matthew M. Heberling for help with analytics.

REFERENCES

(1) Walker, K. D.; Klettke, K.; Akiyama, T.; Croteau, R. *J. Biol. Chem.* **2004**, *279*, 53947–53954.

(2) Jin, M.; Fischbach, M. A.; Clardy, J. *J. Am. Chem. Soc.* **2006**, *128*, 10660–10661.

(3) Huang, X.; Brien, E. O.; Thai, F.; Cooper, G. *Org. Process Res. Dev.* **2010**, *14*, 592–599.

(4) Ruf, S.; Buning, C.; Schreuder, H.; Horstick, G.; Linz, W.; Olpp, T.; Pernerstorfer, J.; Hiss, K.; Kroll, K.; Kannt, A.; Kohlmann, M.; Linz, D.; Hübschle, T.; Rütten, H.; Wirth, K.; Schmidt, T.; Sadowski, T. *J. Med. Chem.* **2012**, *55*, 7636–7649.

(5) Dunn, C. J.; Faulds, D. *Drugs* **2000**, *60*, 607–617.

(6) Kálai, T.; Altenbach, C.; Cascio, D.; Peters, F. B.; Hideg, K.; Schultz, P. G.; Bonneville, J.; Tichtinsky, G.; Von, D.; Springer, A.; Reinbothe, S. *Proc. Natl. Acad. Sci. U.S.A.* **2010**, *107*, 21637–21642.

(7) Peters, F. B.; Brock, A.; Wang, J.; Schultz, P. G. *Chem. Biol.* **2009**, *16*, 148–152.

(8) Aguilar, M.-I.; Purcell, A. W.; Devi, R.; Lew, R.; Rossjohn, J.; Smith, A. I.; Perlmutter, P. *Org. Biomol. Chem.* **2007**, *5*, 2884–2890.

(9) Steer, D. L.; Lew, R. A.; Perlmutter, P.; Smith, A. I.; Aguilar, M.-I. *Curr. Med. Chem.* **2002**, *9*, 811–822.

(10) (a) Turner, N. J. *Curr. Opin. Chem. Biol.* **2011**, *15*, 234–240. (b) Heberling, M. M.; Wu, B.; Bartsch, S.; Janssen, D. B. *Curr. Opin. Chem. Biol.* **2013**, *17*, 250–260.

(11) Poppe, L. *Curr. Opin. Chem. Biol.* **2001**, *5*, 512–524.

(12) Gloge, A.; Zoń, J.; Kövári, A.; Poppe, L.; Rétey, J. *Chem. - Eur. J.* **2000**, *6*, 3386–3390.

DOI: 10.1021/jacs.5b07326
J. Am. Chem. Soc. 2015, 137, 12977–12983

(13) De Lange, B.; Hyett, D. J.; Maas, P. J. D.; Mink, D.; van Assema, F. B. J.; Sereinig, N.; de Vries, A. H. M.; de Vries, J. G. *ChemCatChem* **2011**, *3*, 289−292.
(14) (a) Parmeggiani, F.; Lovelock, S. L.; Weise, N. J.; Ahmed, S. T.; Turner, N. J. *Angew. Chem., Int. Ed.* **2015**, *54*, 4608−4611. (b) Lovelock, S. L.; Lloyd, R. C.; Turner, N. J. *Angew. Chem., Int. Ed.* **2014**, *53*, 4652−4656.
(15) Szymanski, W.; Wu, B.; Weiner, B.; de Wildeman, S.; Feringa, B. L.; Janssen, D. B. *J. Org. Chem.* **2009**, *74*, 9152−9157.
(16) Bartsch, S.; Wybenga, G. G.; Jansen, M.; Heberling, M. M.; Wu, B.; Dijkstra, B. W.; Janssen, D. B. *ChemCatChem* **2013**, *5*, 1797−1802.
(17) Wu, B.; Szymański, W.; Wybenga, G. G.; Heberling, M. M.; Bartsch, S.; de Wildeman, S.; Poelarends, G. J.; Feringa, B. L.; Dijkstra, B. W.; Janssen, D. B. *Angew. Chem., Int. Ed.* **2012**, *51*, 482−486.
(18) Xiang, L.; Moore, B. S. *J. Biol. Chem.* **2002**, *277*, 32505−32509.
(19) Xiang, L.; Moore, B. S. *J. Bacteriol.* **2005**, *187*, 4286−4289.
(20) Chesters, C.; Wilding, M.; Goodall, M.; Micklefield, J. *Angew. Chem., Int. Ed.* **2012**, *51*, 4344−4348.
(21) Magarvey, N. A.; Fortin, P. D.; Thomas, P. M.; Kelleher, N. L.; Walsh, C. T. *ACS Chem. Biol.* **2008**, *3*, 542−554.
(22) Ratnayake, N. D.; Wanninayake, U.; Geiger, J. H.; Walker, K. D. *J. Am. Chem. Soc.* **2011**, *133*, 8531−8533.
(23) Strom, S.; Wanninayake, U.; Ratnayake, N. D.; Walker, K. D.; Geiger, J. H. *Angew. Chem., Int. Ed.* **2012**, *51*, 2898−2902.
(24) Segala, M.; Takahata, Y.; Chong, D. P. *J. Mol. Struct.: THEOCHEM* **2006**, *758*, 61−69.
(25) Ratnayake, N. D.; Liu, N.; Kuhn, L. A.; Walker, K. D. *ACS Catal.* **2014**, *4*, 3077−3090.
(26) Bartsch, S.; Bornscheuer, U. T. *Protein Eng., Des. Sel.* **2010**, *23*, 929−933.
(27) Wanninayake, U.; Walker, K. D. *J. Am. Chem. Soc.* **2013**, *135*, 11193−11204.
(28) Studier, F. W. *Protein Expression Purif.* **2005**, *41*, 207−234.

DOI: 10.1021/jacs.5b07326
J. Am. Chem. Soc. 2015, 137, 12977−12983